Science of the Total Environment 628–629 (2018) 650–660

Contents lists available at ScienceDirect

Science of the Total Environment

journal homepage: www.elsevier.com/locate/scitotenv

Less sensitive of urban surface to climate variability than rural in Northern China

Rui Yao [a], Lunche Wang [a,d,*], Xin Huang [b,c,**], Jiangping Chen [c,d], Jiarui Li [a], Zigeng Niu [a]

[a] Laboratory of Critical Zone Evolution, School of Earth Sciences, China University of Geosciences, Wuhan 430074, China
[b] State Key Laboratory of Information Engineering in Surveying, Mapping and Remote Sensing, Wuhan University, Wuhan 430079, China
[c] School of Remote Sensing and Information Engineering, Wuhan University, Wuhan 430079, China
[d] Key Laboratory for National Geography State Monitoring (National Administration of Surveying, Mapping and Geoinformation), China

HIGHLIGHTS

- SUHII in summer days and winter days was significantly negatively correlated with background LST
- The SUHII generally decreased in hot summers, while increased in cold winters
- The standard deviations were used to reflect the interannual stabilities of LST, EVI and WSA
- Urban LST, EVI and WSA (in winter) were generally more stable than in rural areas.

GRAPHICAL ABSTRACT

The land surface temperature in summer days and winter days in urban cores was more stable than rural in Northern China.

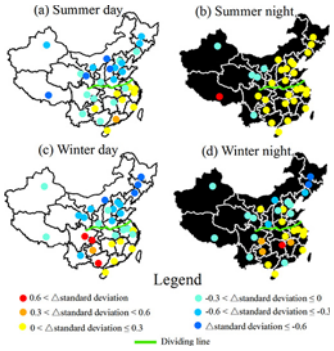

ARTICLE INFO

Article history:
Received 29 November 2017
Received in revised form 1 February 2018
Accepted 8 February 2018
Available online xxxx

Editor: Ouyang Wei

Keywords:
Surface urban heat island
Climate variability
Sensitivity
China

ABSTRACT

In this study, the relationships between interannual variations of surface urban heat islands (SUHIs) and climate variability were studied in 31 cities of China for the period 2001–2016. For cold and dry Northern China, it was found that the interannual variations of SUHI intensity (SUHII, land surface temperature (LST) in urban minus rural) in urban cores was significantly ($p < 0.05$) and negatively correlated with rural LST in 9 (in summer days (SDs)) and 8 (in winter days (WDs)) of the 15 northern cities, respectively. In addition, the daytime LST differences between hot summers and other summers and between cold winters and other winters were generally lower in urban cores (1.141 °C for SDs and 2.535 °C for WDs) than in rural areas (1.890 °C for SDs and 3.377 °C for WDs). The standard deviation was further used to reflect the interannual stabilities of LST, enhanced vegetation index (EVI) and white sky albedo (WSA). Interestingly, the standard deviations of LST across 2001–2016 were generally lower in urban cores (0.994 °C for SDs and 1.577 °C for WDs) than in rural areas (1.431 °C for SDs and 2.077 °C for WDs). Similar results were observed for EVI and WSA (winter). The results suggested that the urban surface is less sensitive to climate variability than rural areas in Northern China. Comparatively, most findings were less evident in hot and humid Southern China. Despite the whole world would become warmer or colder in future, the insensitivity of urban surface may mitigate its impacts in cold and dry Northern China. However, it does not mean that urbanization is totally good due to its environmental problem.

* Correspondence to: L. Wang, Laboratory of Critical Zone Evolution, School of Earth Sciences, China University of Geosciences, Wuhan 430074, China.
** Correspondence to: X. Huang, State Key Laboratory of Information Engineering in Surveying, Mapping and Remote Sensing, Wuhan University, Wuhan 430079, China.
E-mail addresses: wang@cug.edu.cn (L. Wang), Xhuang@whu.edu.cn (X. Huang).

https://doi.org/10.1016/j.scitotenv.2018.02.087
0048-9697/

1. Introduction

One of the important issues that human being is facing is the rapid urbanization, especially in developing countries (United Nations, 2014). A major effect of urbanization is urban heat island (UHI), which refers to higher temperature (including both land surface and air temperatures) in urban area than in rural surrounding and is a prevalent phenomenon that has been observed in hundreds of cities (Peng et al., 2012; Santamouris, 2015). UHIs has many negative impacts on human beings and surface environment: a) it can affect human health, for example, increasing the natural mortality (Goggins et al., 2012; Mohan and Kandya, 2015); b) it can increase energy consumption by increasing cooling needs in summer (Akbari et al., 1992); and c) it can reduce air and water quality (Grimm et al., 2008). Thus, it is necessary to comprehensively study the UHI, including its magnitude, spatiotemporal variations and driving forces.

Another important problem that human being is facing is climate change. It is generally believed that the earth surface is warming (Brown et al., 2017; Sun et al., 2016; Huang et al., 2017a, 2017b; IPCC, 2015). However, the earth may cool in the future due to reductions in solar activities (Shepherd et al., 2014; Landscheidt, 2003; Nevett, 2016). Although future climate change remains controversial, both extreme high and low temperatures have negative impacts on human beings, for example increasing mortality and energy consumption (Kolokotroni et al., 2012; Linares et al., 2015; Schatz and Kucharik, 2015). Therefore, both climate and UHI can significantly alter the urban thermal environment, and have negative impacts on human society, it is important to systematically study the relationships between them.

However, the relationships were still poorly understood at a regional scale. Certain studies analyzed the relationships between UHI and heatwaves using in situ data or model simulations in single city or a few cities in a small region, the results indicated that the UHI intensity (UHII, urban temperature minus rural) was enhanced by heatwaves, especially at night (Founda et al., 2015; Li et al., 2016; Li et al., 2015; Ramamurthy and Bou-Zeid, 2017; Ramamurthy et al., 2015). For example, Founda et al. (2015) showed a significant amplification of nighttime UHII under heat waves in Athens (Greece); Ramamurthy and Bou-Zeid (2017) showed that the UHII was amplified more strongly during heat waves in bigger cities (e.g. New York City, 2 °C) compared to smaller cities in Western United States. Detailed studies for a large area and across different climate regions are needed. Additionally, few studies have analyzed the relationships between UHI and climate in winter. Schatz and Kucharik (2015) showed that the air UHII in winter was negatively related to the daily minimum temperature in Madison (USA), similar results were found in Northern China according to Yao et al. (2017c), however, they did not find the detailed reasons. Furthermore, data from weather stations have some disadvantages in terms of studying the UHI: a) weather stations are spatially scarce and air temperature data from one or few stations cannot be used to represent the whole city; and b) it is hard to choose a reference rural station that immune to UHI, since most stations are located in urban areas (Sun et al., 2016; Wang F. et al., 2015a; Yao et al., 2017b).

Satellite remote sensing provides a new and objective way to monitor the UHI. It has wide spatial coverage and can cover the whole city. The UHI monitored by satellite remote sensing is called surface UHI (SUHI) since satellite data reflect heat information of land surface. Moderate Resolution Imaging Spectroradiometer (MODIS) LST data have wide coverage and can be easily used to study the UHI at national and continental scales (Imhoff et al., 2010; Wang J. et al., 2015b; Ward et al., 2016; Zhou et al., 2015, 2016a, 2016b), which overcomes the drawback (strait coverage) of traditional methods (in situ measurement and model simulation). For instance, Peng et al. (2012) showed that the SUHI intensity (SUHII, urban LST minus rural) is positive in 92% and 95% of the 419 global big cities for daytime and nighttime, respectively.

China has large temperature and precipitation gradients since it covers a large area for about 9.6 million km^2. In addition, China has undergone rapid urbanization in terms of population growth (United Nations, 2014) and urban expansion (Kuang et al., 2016). All of these make China an ideal region to study the SUHI and its relationships with background climate variability. Thus, this study aims at: a) exploring the correlations between interannual variations of SUHII and climate variability in 31 cities in China for the period 2001–2016; b) analyzing the SUHII and LST changes in hot summers and cold winters; c) studying the stabilities of LST, enhanced vegetation index (EVI) and white sky albedo (WSA) in urban and rural areas. The main novel elements of this study includes: a) systematically analyzing the relationships between SUHII and climate variability for a large area and across different background climate zones; b) comprehensively studying the relationships between SUHII and climate in winter; and c) revealing an interesting characteristic of urban surface: the stabilities of LST, EVI and WSA.

2. Data

In this study, the experiments were performed in Yangtze River Delta urban agglomeration (including Shanghai, Suzhou, Changzhou and Wuxi), Pearl River Delta urban agglomeration (including Shenzhen, Dongguan, Guangzhou, Foshan, Zhongshan, Zhuhai, Xianggang and Jiangmen) and other 29 municipalities or provincial capitals (Fig. 1) (Yao et al., 2017c). Due to different geographical locations and climate, the whole China was divided into southern part (including 15 cities, humid climate) and northern part (including 15 cities, semi-humid, semi-arid and arid climate) using Qinling Mountain-Huaihe River Line (Wang J. et al., 2015b). Because of its special location (away from the Qinling Mountain-Huaihe River line) and plateau climate, Lhasa was not classified into any of them (Fig. 1) (Yao et al., 2017c).

China's Land Use/Cover Datasets (CLUDs, produced from Landsat TM/ETM+ and HJ-1A/1B imagery using human-computer interactive interpretation) in the year 2000, 2005, 2010 and 2015 were used to delineate urban and rural areas in this study. The CLUDs have many advantages, for example, high spatial resolution (30 m), high overall accuracy (over 90%) and long time series (5-year interval since the late 1980s). Detail information (e.g. data processing and accuracy assessment) can be found in Liu et al. (2010), Liu et al. (2014) and Kuang et al. (2016).

Terra MODIS LST data (MOD11A2, 8-day composite, 1 km spatial resolution, version 6, for the period 2001–2016) was used to extract LST in this study. The LST data was retrieved using generalized split-window algorithm and improved by correcting noise due to topographic differences, cloud contamination, and zenith angle changes. The accuracy of this data had been widely validated in a wide range (−10 to 58 °C) and different land cover types (Wan, 2008, 2014). This data had been widely used to study the SUHI (Imhoff et al., 2010; Peng et al., 2012; Zhang et al., 2014; Zhou et al., 2014; Wang J. et al., 2015b; Ward et al., 2016; Yao et al., 2017c). Vegetation information was quantified by MODIS MOD13A3 EVI data (1 km spatial resolution, monthly composite, version 6, for the period 2001–2016), with higher value representing higher vegetation activity (pixels with negative value were considered as water bodies and excluded in this study). In addition, albedo information was derived from MCD43B3 shortwave WSA data (1 km spatial resolution, 8-day composite, version 5, for the period 2001–2016), respectively. Finally, precipitation data for the period 2001–2015 from weather stations (obtained from China Meteorological Administration) in and around the city were used in the present study (Fig. 1). EVI and WSA data had been widely validated and used by previous studies (Liang et al., 2002; Huete et al., 2002; He et al., 2012; Peng et al., 2012; Zhou et al., 2014).

3. Methods

Fig. 3 shows the flow chart of the methodologies in this study. The CLUDs were first merged into three broad types: built-up area

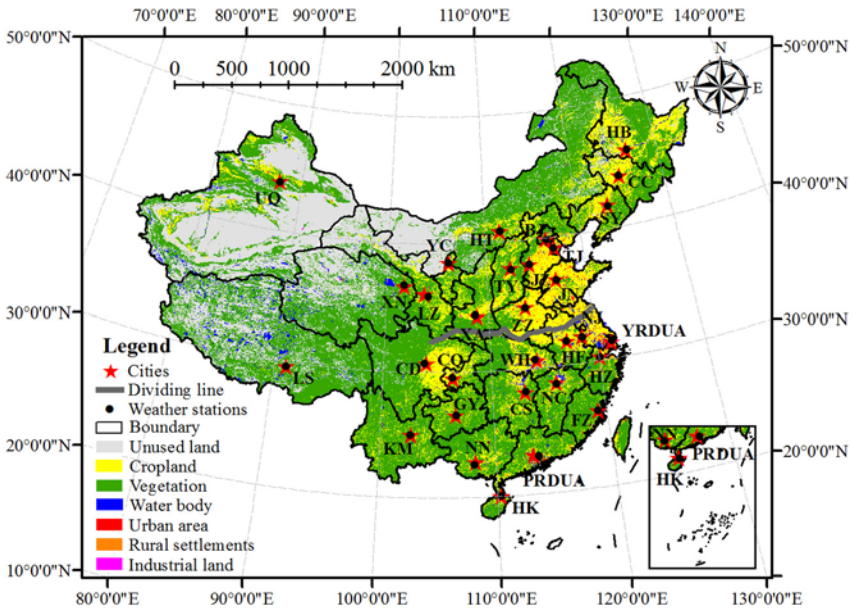

Fig. 1. The 31 cities and weather stations in this study. 15 northern cities: Beijing (BJ), Changchun (CC), Harbin (HB), Jinan (JN), Lanzhou (LZ), Urumqi (UQ), Shenyang (SY), Hohhot (HT), Tianjin (TJ), Yinchuan (YC), Shijiazhuang (SJZ), Taiyuan (TY), Xining (XN), Zhengzhou (ZZ) and Xi'an (XA). 15 southern cities: Changsha (CS), Chengdu (CD), Chongqing (CQ), Fuzhou (FZ), Nanjing (NJ), Yangtze River Delta Urban Agglomeration (YRDUA), Heifei (HF), Hangzhou (HZ), Wuhan (WH), Nanchang (NC), Guiyang (GY), Kunming (KM), Nanning (NN), Pearl River Delta Urban Agglomeration (PRDUA) and Haikou (HK). Plateau city: Lhasa (LS).

(including urban area, industrial land and rural settlement), water body and other types (including cropland, forest, grassland and unused land). We then generated resampled maps (1 km spatial resolution, keep accordance with MODIS data) and proportion maps (the proportions of each of the 3 land cover types for each pixel with 1 km spatial resolution). To minimize the influences of interannual urbanization on SUHII, the analyses in this study were only conducted in the intersection area of urban cores (UCs, pixels consisted of 100% of the built-up area; Fig. 2) in all four CLUDs (in the year 2000, 2005, 2010, 2015) (Cao et al., 2016). In other words, this study only performed in fixed urban area throughout the whole study period. Additionally, the 20–25 km buffer around the urban area was used as rural reference (excluding pixels with water body higher than 0% or built-up area higher than 5%; Fig. 2) (Imhoff et al., 2010; Yao et al., 2017a, 2017c; Zhou et al., 2016c). In the present study, the rural references were far from urban areas, since the SUHI's footprint was far greater than urban area size according to Zhang et al. (2004), Han and Xu (2013) and Zhou et al. (2015). This study did not exclude the impacts of elevation, the reasons can be found in supporting information.

MOD11A2 data detected at 10: 30 am and 10: 30 pm (local solar time) were used to represent daytime and nighttime LSTs, respectively. Then they were averaged into summer (defined as June, July and August) and winter (defined as December, January and February). Thus, the analyses of this study were performed in four time periods: summer days (SDs), summer nights (SNs), winter days (WDs) and winter nights (WNs).

Eq. (1) was used to compute the SUHII (Peng et al., 2012; Yao et al., 2017a):

$$\triangle \mathrm{LST}\ (\mathrm{SUHII}) = \mathrm{LST}_{\mathrm{UC}} - \mathrm{LST}_{\mathrm{rural}} \quad (1)$$

where the $\mathrm{LST}_{\mathrm{UC}}$ and $\mathrm{LST}_{\mathrm{rural}}$ are the LSTs in UC and rural area, respectively. Thus the △LST is the SUHII in UC. Moreover, the △EVI and △WSA were computed using the same way as Eq. (1).

The experiments include three main sections:

(1) Exploring the relationships between SUHII and climate variability in each city. The LST averaged for daytime and nighttime in rural area (background LST, henceforth) was used to reflect background climate variability of a city (Yao et al., 2017c). We did not use in situ data, since most of the weather stations are situated in urban areas and it is hard to select a rural station that immune to UHI (Sun et al., 2016; Wang F. et al., 2015a). Pearson's correlation analyses were employed to analyze the relationships between SUHII and background LST in each city across 2001–2016. Note that the correlation analyses in this study were performed across time (years), which were different from space (cities) in previous studies (Imhoff et al., 2010; Peng et al., 2012; Clinton and Gong, 2013; Wang J. et al., 2015b; Du et al., 2016; Zhou et al., 2014, 2016b).

(2) Analyzing the changes in LST and SUHII in hot summers and cold winters in each city. The heat magnitude (HM) and the cold magnitude (CM) was used to analyze the changes in LST in hot summers and cold winters, respectively:

$$\mathrm{HM} = \mathrm{LST}_{\text{hot summers}} - \mathrm{LST}_{\text{other summers}} \quad (2)$$

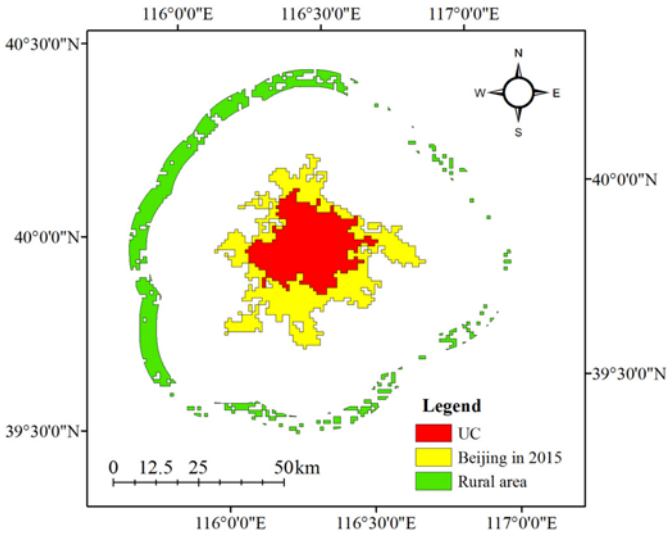

Fig. 2. The schematic diagram of urban core (UC) and rural area in Beijing.

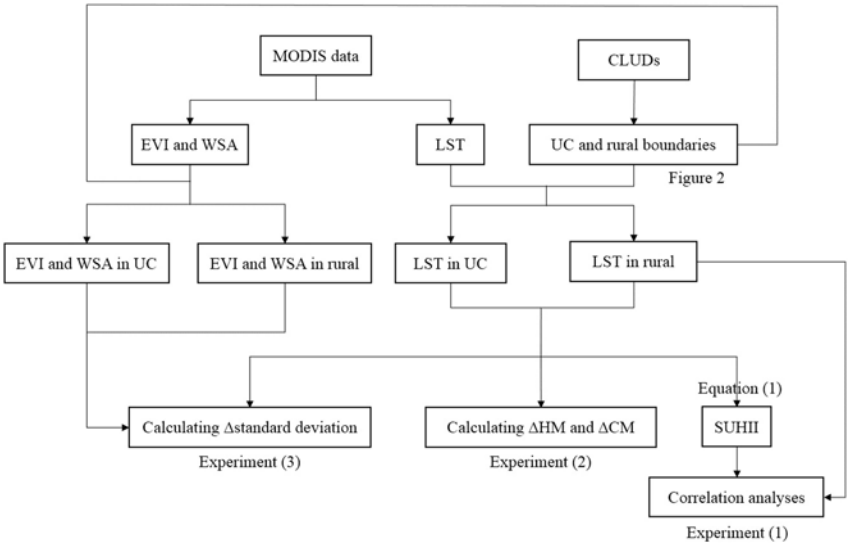

Fig. 3. The flow chart of the methodologies in this study.

$$CM = LST_{\text{cold winters}} - LST_{\text{other winters}} \quad (3)$$

where the $LST_{\text{hot summers}}$ and the $LST_{\text{other summers}}$ represent the average LST in the hottest three summers and other 13 summers for the period 2001–2016, respectively. The hottest three summers of a city were defined as summers with the highest, the second highest and the third highest background LST. Note that these hot summers somewhat varied among the 31 cities. Thus the HM represents the average LST difference between the hottest three summers and the other summers. We used three summers rather than one or two to minimize the influences of climate variability, human activity and data quality (Imhoff et al., 2010; Zhang et al., 2014; Zhou et al., 2016b). The $LST_{\text{cold winter}}$ and the

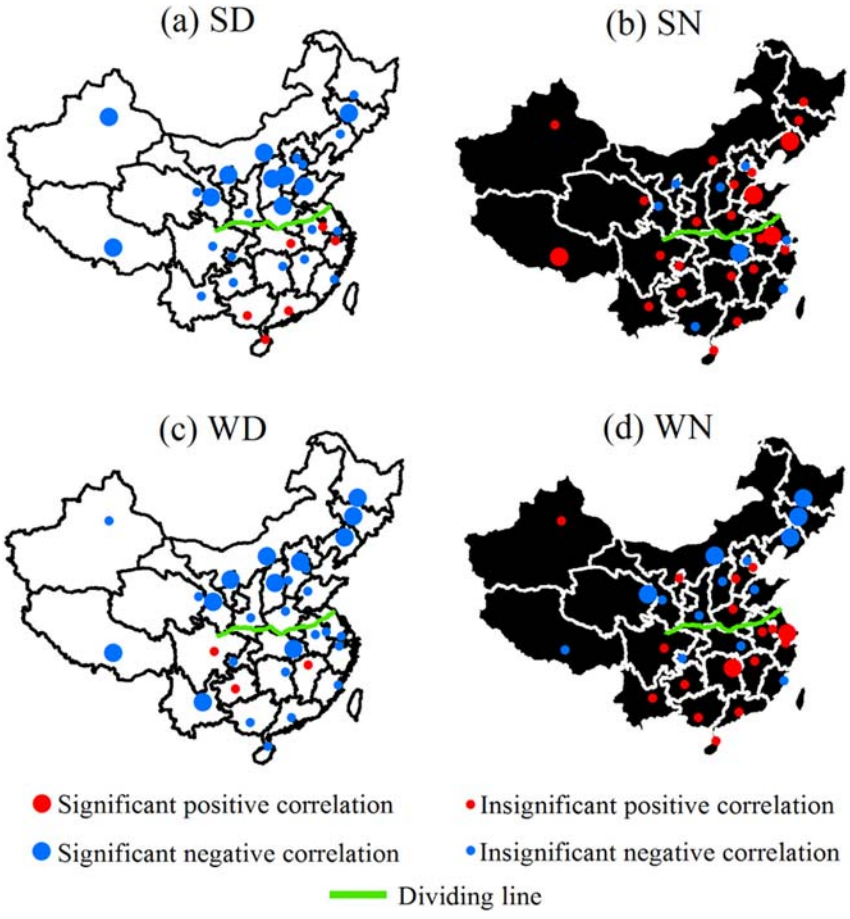

Fig. 4. Pearson's correlation analyses between background land surface temperature (LST) and surface urban heat island intensity (SUHII) in (a) summer days (SDs); (b) summer nights (SNs); (c) winter days (WDs) and (d) winter nights (WNs).

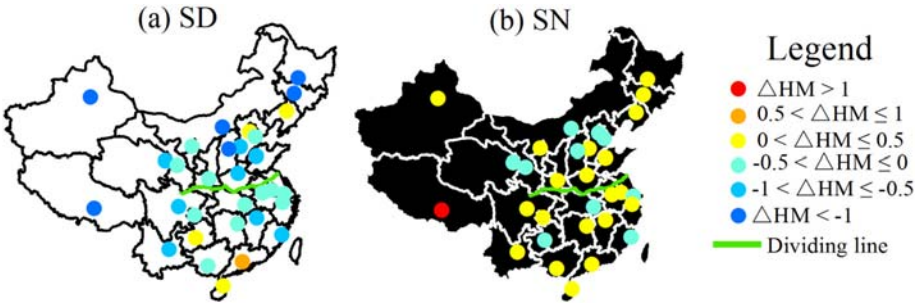

Fig. 5. The △heat magnitudes (HMs) in (a) SDs and (b) SNs.

$LST_{other\ winter}$ represent the average LST in the coldest three winters and other 13 winters, respectively. The coldest three winters of a city were defined as winters with the lowest, the second lowest and the third lowest background LST. Thus the CM represents the average LST difference between the coldest three winters and the other winters. Additionally, the △HM and △CM were calculated as Eqs. (4) and (5), respectively:

$$\triangle HM = HM_{UC} - HM_{rural} \quad (4)$$

$$\triangle CM = CM_{UC} - CM_{rural} \quad (5)$$

where the HM_{UC} and the HM_{rural} are the HM in UC and rural area, respectively. If the △HM was greater than zero, it suggested that in hot summers, the increase in LST was more in UC than in rural area and the SUHII increased (and vice versa). If the △CM was greater than zero, it suggested that in cold winters, the decrease in LST in cold winters was less in UC than in rural area and the SUHII increased (and vice versa).

(3) Studying the stabilities of LST, EVI and WSA in each city. We used the standard deviation (σ) to reflect the stability of LST:

$$\sigma = \sqrt{\frac{1}{16}\sum_{i=2001}^{2016}(LST_i - u)^2} \quad (6)$$

where the LST_i is the LST in the year i, u is the average LST for the whole study period. The standard deviation of LST was calculated for each pixel separately. The standard deviation of LST in UC was computed as the average standard deviation of all pixels in UC (the same as rural area). The standard deviations of EVI and WSA were calculated using the same method as Eq. (6). In addition, the △σ was calculated using Eq. (7):

$$\Delta\sigma = \sigma_{UC} - \sigma_{rural} \quad (7)$$

where the σ_{UC} and the σ_{rural} are the σ in UC and rural area, respectively. If the △σ was less than zero, it suggested that the LST (or EVI or WSA) in UC was more stable and less sensitive to climate variability than in rural area across 2001–2016 (and vice versa).

There are many gaps in MCD43B3 WSA data. Therefore, the years with proportion of gaps higher than 20% in UC or rural area were excluded in each city (Hu et al., 2016; Weng and Fu, 2014). Cities with proportion of invalid years higher than 4 years (>20%) were excluded in this study.

The monitoring time of MYD11A2 data (Aqua satellite, 1:30 am and 1:30 pm on local solar time) was different from MOD11A2 data (Terra satellite). Therefore, we used the MYD11A2 data (for the period 2003–2016) as a supplement. The experiments in this study were performed using MOD11A2 and MYD11A2 data separately. All of the results observed by Aqua satellite can be found in supporting information.

4. Results

4.1. The relationships between SUHII and background climate variability

Background climate variability has great impacts on interannual variations in SUHII on SDs and WDs in Northern China (Fig. 4). The SUHII was negatively correlated with the background LST in all of the northern cities in SDs and WDs, over half of the northern cities showed significant ($p < 0.05$) negative correlations (Fig. 4). Similarly, the plateau city (Lhasa) also presented significant negative correlation between SUHII and background LST on SDs and WDs. However, most cities in Southern China exhibited insignificant correlations (Fig. 4).

The SUHII in SNs was generally invariant with background climate, the significant correlations were only found in few cities (Fig. 4). Additionally, there were 5 of 15 northern cities exhibiting significant negative correlations between SUHII and background LST on WNs. Finally, all of the results observed by Terra satellite were similar to Aqua satellite (Fig. S1).

4.2. The HM in hot summers and the CM in cold winters

The increase in daytime LST in hot summers was generally lower in UCs than in rural areas, as the △HM were less than zero in most cities (26 of 31 cities), especially in Northern China (15 of 15 cities, Fig. 5). In other words, the daytime SUHII decreased in hot summers in most

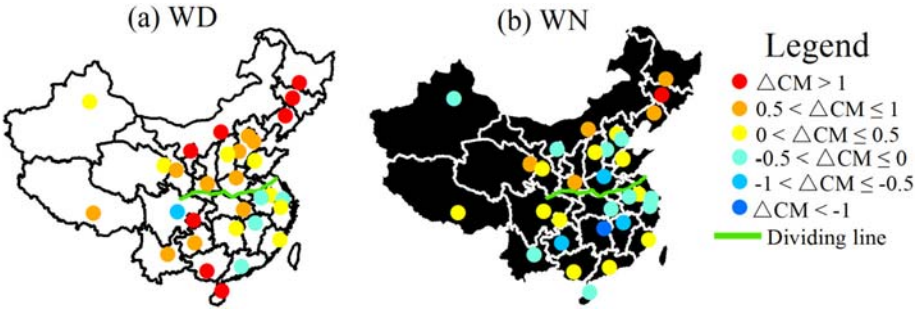

Fig. 6. The △cold magnitudes (CMs) on (a) WDs and (b) WNs.

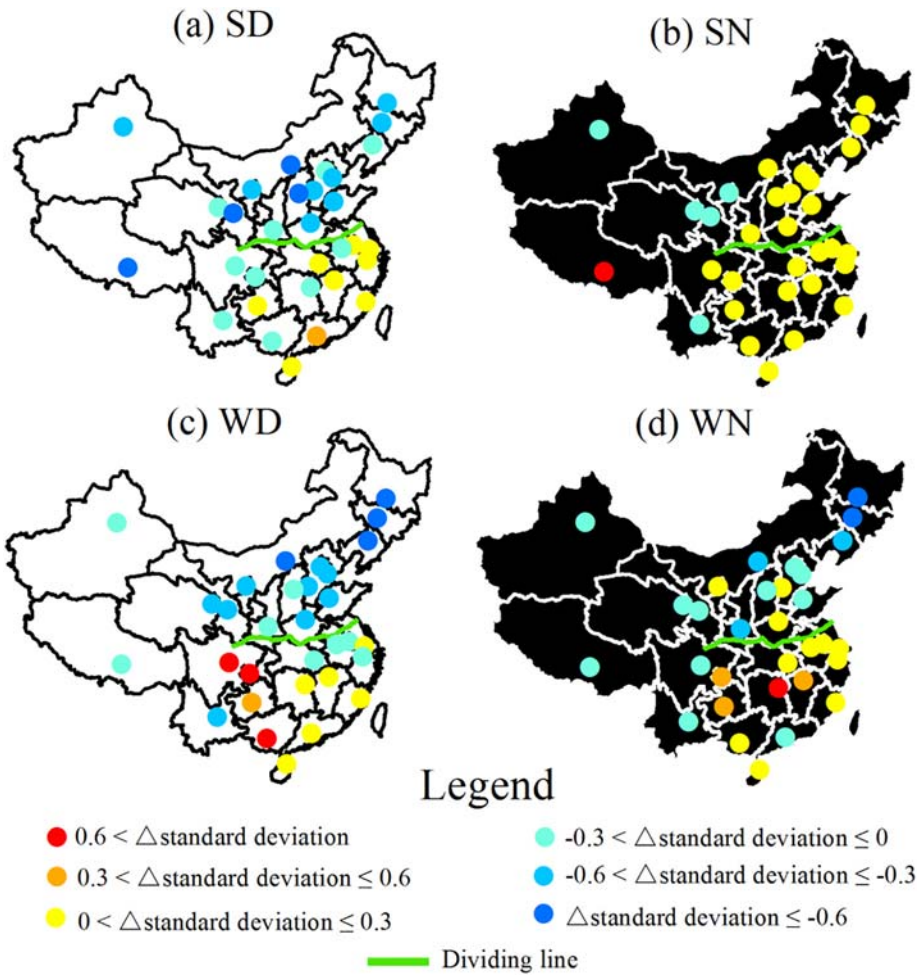

Fig. 7. The △standard deviations of LST in (a) SDs; (b) SNs; (c) WDs and (d) WNs.

cities. For all cities combined, the HM on SDs in UC was 1.072 °C, which was lower than in rural area (1.577 °C; Table 1). It suggested that the daytime SUHII in hot summers was 0.505 °C lower than other summers. These were more prominent in Northern China (UC: 1.141 °C, rural: 1.890 °C; Table 1). On the contrary, for 31 cities averaged, the HM on SNs was a little higher in UC (0.843 °C) than in rural area (0.720 °C). It means that the nighttime SUHII in hot summers was 0.123 °C higher than other summers. Moreover, for 31 cities combined, the HM on SNs (UC: 0.843 °C; rural: 0.720 °C) was lower than in SDs (UC: 1.072 °C; rural: 1.577 °C; Table 1).

In cold winters during the daytime, the decreases in LST were normally less in UCs than in rural areas, as the △CM was greater than zero in 26 of 31 cities, particularly for Northern China (15 of 15 cities; Fig. 6). It suggested that the daytime SUHII generally increased in cold

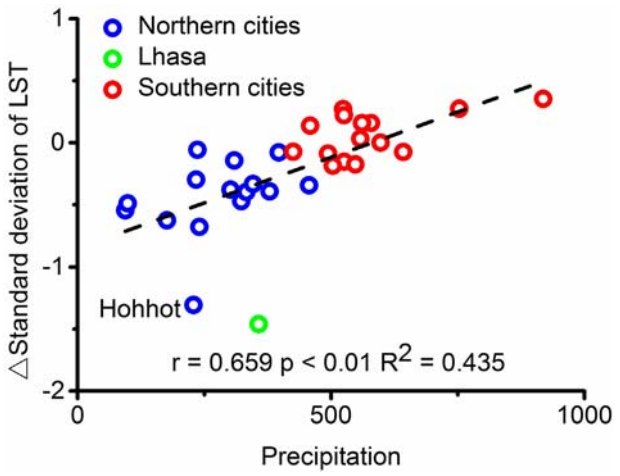

Fig. 8. Pearson's correlation analyses between precipitation and △standard deviation of LST on SDs across 31 cities in China.

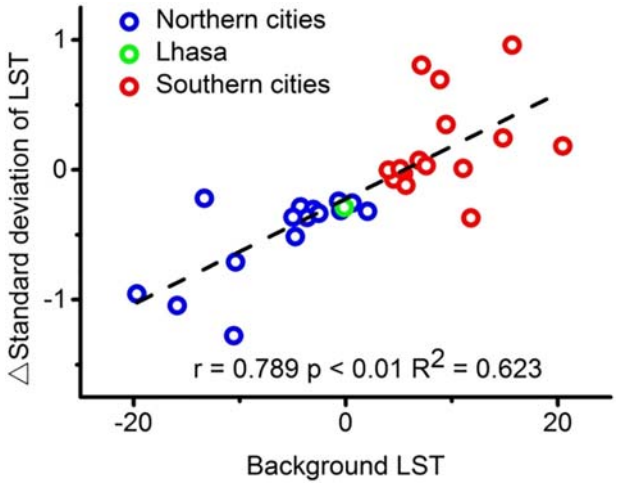

Fig. 9. Pearson's correlation analyses between background LST and △standard deviation of LST on WDs across 31 cities in China.

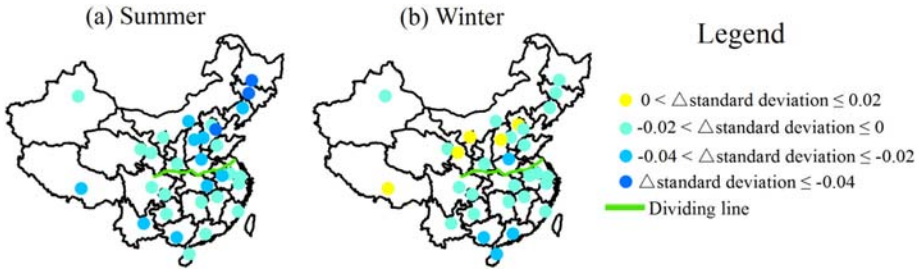

Fig. 10. The △ standard deviations of enhanced vegetation index (EVI) in (a) summer and (b) winter in China across 2001–2016.

winters. For all cities combined, the CM in WDs in UC (−2.130 °C) was higher than in rural area (−2.756 °C; Table 1). In other words, the SUHII was 0.626 °C higher in cold winters than other winters. It was more evident in Northern China (UC: −2.535 °C; rural: −3.377 °C). In addition, the higher CM in UC than in rural area was also observed in WNs in Northern China (UC: −2.385 °C; rural: −2.733 °C). Spatially, the CM averaged for northern cities was lower than southern cities in both WDs and WNs (Table 1). The △HM and △CM in Lhasa were similar to northern cities (Figs. 5 and 6). Finally, all of the results observed by Terra satellite were consistent with Aqua satellite (Figs. S2 and S3).

4.3. Less sensitive of LST to climate variability in UC than rural in Northern China

In Northern China, the LST in SDs and WDs across 2001–2016 was normally more stable and less sensitive to climate variability in UCs than in rural areas (Fig. 7). The standard deviations of LST in UCs were lower than in rural areas in all of the northern cities in SDs (Fig. 7a). For 15 northern cities combined, the standard deviation of LST in SDs in UC (0.994 °C) was much lower than in rural area (1.431 °C). However, the opposite results were found in southern cities: a) the numbers of cities with △ standard deviation of LST higher and lower than zero were 9 and 6, respectively, and b) for 15 southern cities combined, the standard deviation of LST in SDs in UC (1.050 °C) was nearly equal to rural area (0.993 °C).

In WDs, all northern cities showed lower standard deviations of LST in UCs than in rural areas (Fig. 7c). The standard deviation of LST averaged for 15 northern cities in WDs in UC (1.577 °C) was much lower than in rural area (2.077 °C) (Table 2). However, these were different from southern cities: a) the number of cities with △ standard deviation of LST higher or lower than zero were 10 and 5, respectively; and b) for 15 southern cities averaged, the standard deviation of LST in WDs in UC (1.689 °C) was a little higher than in rural area (1.504 °C).

We used the precipitation (in summer averaged for 2001–2015) and background LST (in winter averaged for 2001–2016) to reflect the background climate of a city. Correlation analyses between precipitation or background LST and △standard deviation of LST were performed across 31 cities to explain the spatial variations in stability of LST. It was found that drier (northern) cities usually showed lower △standard deviation of LST in SDs, since the △standard deviation of LST was significantly ($p < 0.01$) and positively ($r = 0.659$) related to precipitation across 31 cities (Fig. 8). In addition, there were two outliers (Hohhot and Lhasa) in the correlation analyses (Fig. 8). Furthermore, colder (northern) cities normally presented lower △standard deviation of LST in WDs, as the △standard deviation of LST was significantly ($p < 0.01$) and positively ($r = 0.789$) correlated with background LST across 31 cities (Fig. 9).

In SNs, the LST in UCs was more sensitive to climate variability than in rural areas in 26 out of 31 cities (Fig. 7b). However, the differences in △standard deviations of LST in SNs between UCs and rural areas were usually small (<0.3 °C; Fig. 7b). For 31 cities combined, the standard deviation of LST in SNs in UC was 0.839 °C, which was a little higher than in rural area (0.726 °C, Table 2). In WNs, the standard deviation of LST averaged for 15 northern cities was 1.415 °C in UC, which was lower than in rural area (1.648 °C). The reverse results were found in Southern China (UC: 1.366 °C, rural: 1.199 °C). Furthermore, Lhasa exhibited similar results with northern cities (Fig. 7). Finally, all findings observed by Terra satellite were similar to Aqua satellite (Fig. S4).

4.4. Less sensitive of EVI and WSA to climate variability in UC than rural in Northern China

Interestingly, the standard deviations of EVI in summer were lower in UCs than in rural areas in all of the 31 cities (Fig. 10a). It suggested that the EVI in summer was more stable and less sensitive to climate variability in UCs than in rural areas. For 31 cities averaged, the standard deviation of EVI in summer in UC was 0.0248, which was much lower than in rural area (0.0443; Table 3). These were more prominent in Northern China (UC: 0.0215, rural: 0.0465; Table 3). In contrast, these phenomena were more evident in Southern China than Northern China in winter: a) the △standard deviations of EVI were less than zero in all of the southern cities and in 11 of 15 northern cities (Fig. 10b); and b) the △standard deviation of EVI averaged for northern cities was −0.0058, which was much higher than southern cities (−0.0145; Table 3).

The △standard deviations of WSA were only analyzed in the minority of the cities due to a great number of gaps in the MCD43B3 product. The interesting findings were that all of the 8 cities in winter showed lower standard deviations of WSA in UCs than in rural areas (Fig. 11b). For 8 cities combined, the △standard deviation of WSA was −0.0229 (UC: 0.0183, rural: 0.0412). It suggested that the WSA in

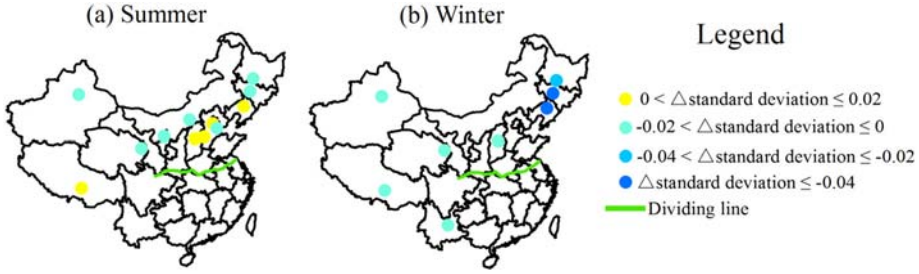

Fig. 11. The △standard deviations of white sky albedo (WSA) in (a) summer and (b) winter in China across 2001–2016.

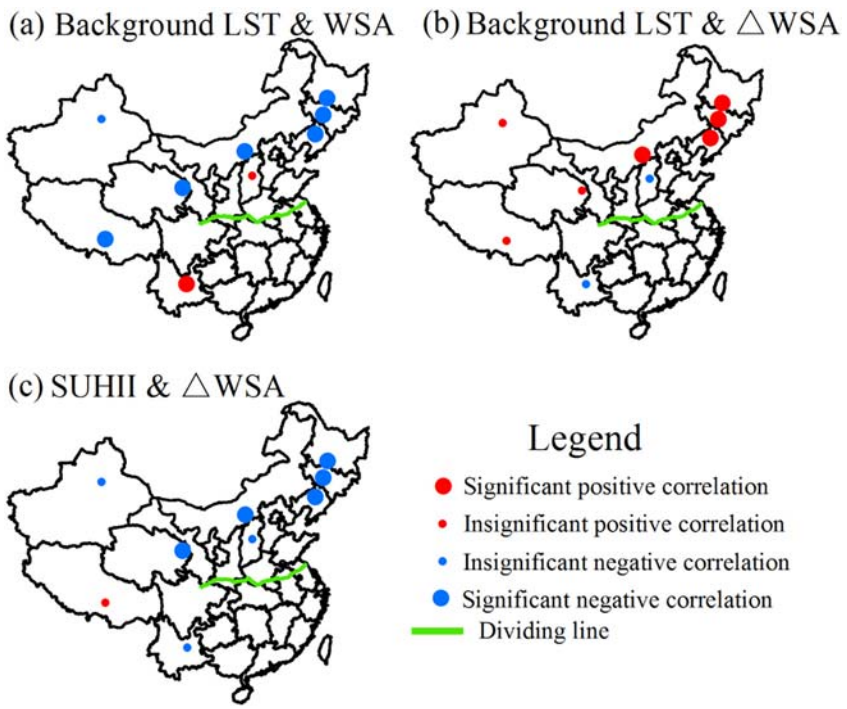

Fig. 12. The Pearson's correlation analyses between (a) LST and WSA in rural area; (b) LST in rural area and △WSA; (c) SUHII and △WSA.

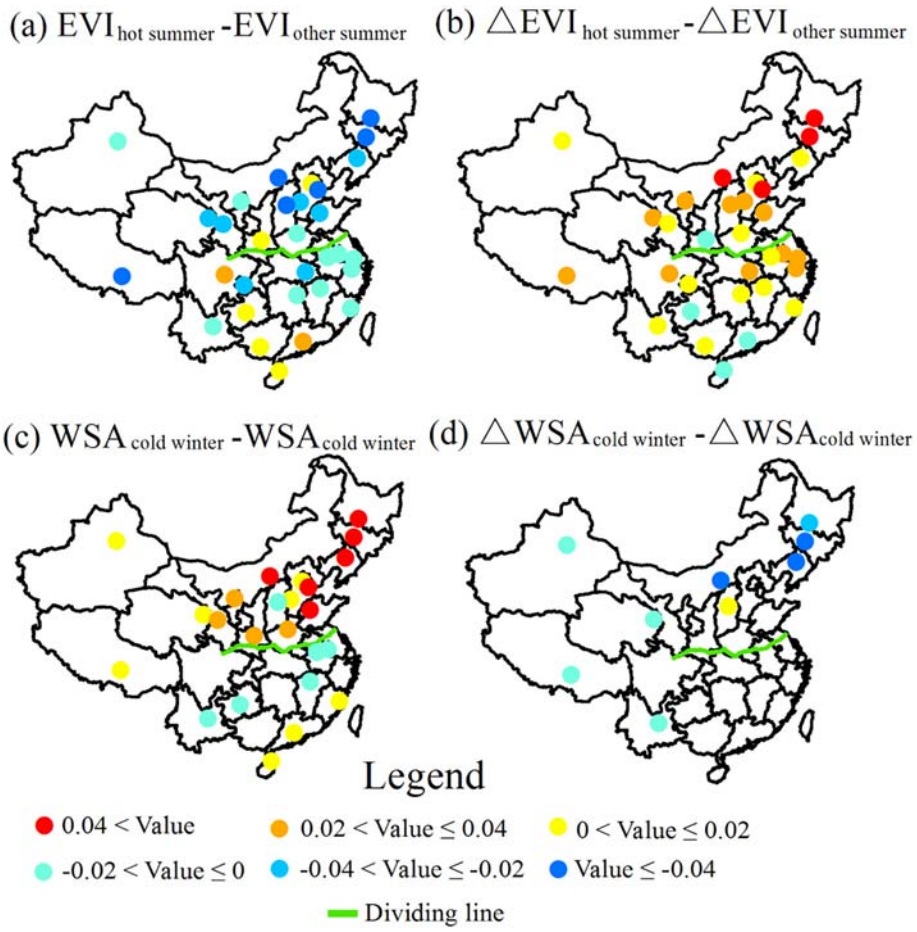

Fig. 13. (a) The EVI difference between hot summers ($EVI_{hot\ summer}$) and other summers ($EVI_{other\ summer}$); (b) the △EVI difference between hot summers ($\triangle EVI_{hot\ summer}$) and other summers ($\triangle EVI_{other\ summer}$); (c) The WSA difference between hot summers and other summers; (d) the △WSA difference between hot summers and other summers.

Table 1
The heat magnitudes (HMs) and cold magnitudes (CMs) averaged for southern cities, northern cities and 31 cities in China. SD: summer day, SN: summer night, WD: winter day, WN: winter night, UC: urban core.

	SD		SN	
HM	UC	Rural area	UC	Rural area
Northern cities	1.141 °C	1.890 °C	0.637 °C	0.565 °C
Southern cities	0.834 °C	1.001 °C	0.887 °C	0.798 °C
31 cities in China	1.072 °C	1.577 °C	0.843 °C	0.720 °C
	WD		WN	
CM	UC	Rural area	UC	Rural area
Northern cities	−2.535 °C	−3.377 °C	−2.385 °C	−2.733 °C
Southern cities	−1.804 °C	−2.198 °C	−2.080 °C	−1.908 °C
31 cities in China	−2.130 °C	−2.756 °C	−2.195 °C	−2.284 °C

winter in UCs was more stable than in rural areas. However, these were less evident in summer: a) the numbers of cities with △standard deviation of WSA higher and lower than zero were 5 and 7, respectively (Fig. 11a); and b) for 12 cities averaged, the △standard deviation of WSA was 0.00014 (UC: 0.00788, rural: 0.00774).

5. Discussion

5.1. The relationships between background LST and SUHII

In the present study, over half of the northern cities presented significant negative correlations between SUHII and background LST in SDs (Fig. 4). These can be explained by vegetation and soil moisture. In summer, elevated LST in rural areas can decrease the soil moisture, then increase the increasing rate of LST in rural area during the daytime and finally decrease the SUHII (Winguth and Kelp, 2013; Yao et al., 2017c). In addition, high temperature and low soil moisture were harmful to vegetation growth in semi-arid and arid region, for example, most parts of the Northern China (Piao, 2003). The decreasing EVI can increase the LST in rural area and then decrease the SUHII, since vegetation can pose a cooling effect (Haashemi et al., 2016; Peng et al., 2012; Taheri Shahraiyni et al., 2016). These mechanisms were demonstrated by Yao et al. (2017c). Spatially, Lhasa also showed significant negative correlation between SUHII and background LST on SDs, probably because the similar background climate (dry) between Lhasa and northern cities (Fig. 8). In Southern China, no cities presented significant negative correlations, probably because the abundant precipitation and saturated soil moisture in summer.

In over half of the northern cities, the SUHII on WDs was significantly and negatively correlated with background LST (Fig. 4). These were similar to Schatz and Kucharik (2015) and Yao et al. (2017c). These can be explained by albedo effects. In rural areas, a reduction in LST can increase the snow and ice in winter, thus increase albedo since ice and snow have higher albedo than other land cover types. The snow and ice can reflect more sunlight and further decrease the LST in rural areas. On the contrary, snow and ice in UCs are often removed by human beings. Thus the △WSA will decrease and then the SUHII will increase. These can be demonstrated by a series of correlation analyses: a) in most cities, the background LST was negatively and positively related to the WSA (in rural areas; Fig. 12a) and △WSA (Fig. 12b), respectively; and b) in most cities, the SUHII in WDs was negatively related to the △WSA (Fig. 12c). Spatially, Lhasa also exhibited significant negative correlations, probably because the similar background climate (cold) between Lhasa and northern cities (Fig. 9). In Southern China, few cities showed significant negative correlations between SUHII and background LST in WDs, mostly owing to warm climate (Fig. 9).

Table 2
The standard deviation of land surface temperature (LST) averaged for southern cities, northern cities and 31 cities in China.

	SD		SN	
Standard deviation	UC	Rural area	UC	Rural area
Northern cities	0.994 °C	1.431 °C	0.761 °C	0.697 °C
Southern cities	1.050 °C	0.993 °C	0.797 °C	0.688 °C
31 cities in China	1.060 °C	1.291 °C	0.839 °C	0.726 °C
	WD		WN	
Standard deviation	UC	Rural area	UC	Rural area
Northern cities	1.577 °C	2.077 °C	1.415 °C	1.648 °C
Southern cities	1.689 °C	1.504 °C	1.366 °C	1.199 °C
31 cities in China	1.609 °C	1.771 °C	1.369 °C	1.403 °C

Table 3
The standard deviation of enhanced vegetation index (EVI) averaged for southern cities, northern cities and 31 cities in China.

	Summer		Winter	
Standard deviation	UC	Rural area	UC	Rural area
Northern cities	0.0215	0.0465	0.0097	0.0155
Southern cities	0.0282	0.0423	0.0163	0.0308
31 cities in China	0.0248	0.0443	0.0128	0.0226

5.2. The HM in hot summers and the CM in cold winters

The increase in LST in hot summers was generally higher in rural areas than in UCs in SDs, particularly for Northern China (Fig. 5 and Table 1). These can be attributed to soil moisture and vegetation. We calculated the average EVI (in rural areas) and △EVI (EVI in UC minus rural) differences between hot summers and other summers (the same method as Eq. (2)). The EVI was lower in hot summers than other summers in 24 of 31 cities, particularly for Northern China (13 of 15 cities; Fig. 13a). In addition, the △EVI was higher in hot summers than other summers in 27 of 31 cities, especially in Northern China (14 of 15 cities, Fig. 13b). The increase in △EVI may be one of the reasons for reduction in SUHII in hot summers. In addition, the decreasing SUHII in hot summers during the daytime was different from previous studies, which showed that the UHII increased during heatwaves (Li and Bou-Zeid, 2013; Ramamurthy and Bou-Zeid, 2017; Ramamurthy et al., 2015). These were possibly due to different methods, previous studies compared the UHI between heatwave days and neighboring non-heatwave days in the same year, the vegetation may not change substantially.

The decrease in LST in cold winters was lower in UCs than in rural areas in WDs, particularly for northern cities (Fig. 6 and Table 1). These can be attributed to albedo effects. We analyzed the WSA (in rural area) and △WSA (WSA in UC minus rural) differences between cold winters and other winters (the same method as Eq. (3)). The WSA was higher in cold winters than other winters in 18 of 24 cities, while the △WSA was lower in cold winters than other winter in 8 of 9 cities (Fig. 13). The decreased △WSA may be one of the reasons for the increasing SUHII in cold winters.

For 31 cities combined, the HM in SDs was higher than SNs, especially in rural areas (Table 1). This can be attributed to soil moisture. In hot summers, the decreased soil moisture can increase the changing rate of LST, thus the LST decreased quickly at night and the HM also decreased. Moreover, for 31 cities combined, the HM in SNs in UC was 0.123 °C higher than in rural area (Table 2), it suggested that the nighttime SUHII was 0.123 °C higher in hot summers than in other summers. This was similar to previous studies, which showed that the nighttime air UHI can be strengthened by heatwaves (Founda et al., 2015; Ramamurthy and Bou-Zeid, 2017; Winguth and Kelp, 2013). The decreased soil moisture and increased anthropogenic heat release may play important roles.

5.3. Less sensitive of LST to climate variability in UC than rural in northern cities

In this study, for 15 northern cities averaged, the LST in SDs, WDs and WNs was more stable in UCs than in rural areas. In SDs, the more stable LST in UCs than in rural areas can be explained by soil moisture and vegetation. The soil has high water retention ability. The background climate variability can influence the soil moisture significantly, and the soil moisture may change substantially across years, particularly for drier Northern China (Fig. 8). By contrast, the urban surface has low water retention ability and may often be dry (Du et al., 2016). In addition, the more stable EVI in UCs than in rural areas may also be the reasons for the more stable LST in UCs than in rural areas (Fig. 10), since EVI had been proved strongly correlate with LST (Peng et al., 2012; Weng, 2009; Yao et al., 2017a). In addition, it was clear that the △standard deviation of LST in Hohhot and Lhasa in SDs were lower than other cities (Fig. 8), which can be attributed to the plateau climate of these two cities. The plateau region is sensitive to climate and the standard deviation of LST in SDs in rural areas (Hohhot: 2.594 °C, Lhasa: 3.659 °C) were higher than other cities (other 29 cities averaged: 1.164 °C).

In WDs, the more stable LST in UCs than in rural areas in northern cities can be explained by its cold climate and human activities. Cold cities usually have lower △standard deviation of LST (Fig. 9). Low temperature can increase the snow, ice and WSA. The human activity can lead to more stable WSA in UCs than in rural areas (Fig. 11).

The soil moisture has the opposite effects on LST in SDs and SNs as mentioned in Section 4.2. Thus the correlations, HMs and standard deviations in northern cities in SDs were different from SNs (Figs. 4, 5, 6 and 7). However, the water in the soil was generally replaced by ice and snow in Northern China in WNs. The specific heat capacity of water is much higher than ice, thus the correlations, CMs and standard deviations in northern cities in WNs were similar to WDs (although the results were less prominent on WNs; Figs. 4, 5, 6 and 7).

5.4. Less sensitive of EVI and WSA to climate variability in UC than rural in northern cities

In the present study, the EVI was more stable in UCs than in rural areas (Fig. 10). The amount of vegetation and the EVI were generally higher in rural areas than in UCs. Thus more vegetation will be affected by climate variability and the changes in EVI may be greater in rural areas than in UCs. In addition, the vegetation may be affected by human activity in UCs (e.g. irrigation), thus the influences of climate variability (e.g. high temperature and drought) may be mitigated and the EVI may be more stable in UCs than in rural areas. This phenomenon was less evident in Northern China in winter (Fig. 10b), mostly owing to the vegetation types (larch and seasonal crop) in Northern China (Zhou et al., 2014).

The △standard deviations of WSA were less than zero in all of the 8 cities in winter (Fig. 11b). These can be attributed to human activities. Spatially, this was less obvious in summer, probably because less snow and ice. Finally, Lhasa exhibited similar △standard deviations of LST, EVI and WSA with northern cities, mostly owing to similar background climate (cold and dry) between them (Figs. 8 and 9).

5.5. Possible benefits of the insensitivity of urban surface

This study focused on the LST and SUHII, which were completely different from the air temperature and air UHI. Although human health and comfort may be more affected by air UHI than SUHI (Anniballe et al., 2014; Zhou et al., 2016b), the SUHI was a primary driver of air UHI and closely relating to the air UHI (Clinton and Gong, 2013; Weng, 2009).

The UHI in winter can effectively mitigate the impacts of low temperature, and have some benefits such as reducing heating needs and save lives, especially in cold region such as Northern China (Kolokotroni et al., 2012; Schatz and Kucharik, 2015; Yao et al., 2017c). These positive effects may become more prominent in cold winters when the SUHII increased according to the present study. If the global cooling occurred in future, rapid urbanization may effectively mitigate its impacts. Therefore, in cold regions such as Northern China, people should consider the possible benefits of UHI when designing and applying mitigation strategies of UHI. Moreover, we suggest removing the snow and ice in cold winter, since it can relief the influences of low temperature according to this study.

Dry regions are known to be more sensitive to climate change than humid regions. Global warming over dry regions was much higher than over humid regions over the past century (Huang et al., 2017a, 2017b). Fortunately, in hot summers, the SUHII usually decreased in dry Northern China according to the present study, the impacts of high temperature in UCs may be relieved. In addition, the hotter the summer, the lower the SUHII (Fig. 4). However, rapid urbanization can increase both LST and air temperature in urban areas, increasing the duration and intensity of heatwaves undoubtedly (Luo and Lau, 2017; Schatz and Kucharik, 2015). If the global warming and rapid urbanization continued, people will suffer from more severe heat waves.

6. Conclusions

In this study, the relationships between SUHII or LST and background climate variability were systematically analyzed in 31 cities of China for the period 2001–2016.

For northern cities, the major findings in this study include: (1) The SUHII in SDs and WDs was significantly and negatively related to the background LST in more than half of the northern cities. These can be attributed to vegetation and soil moisture in SDs, and albedo effects in WDs. (2) The HMs in SDs was usually lower in UCs than in rural areas, while the CMs in WDs and WNs was normally higher in UCs than in rural areas. In rural areas, the EVI generally decreased in hot summers and the WSA normally increased in cold winters. (3) The standard deviations of LST in SDs and WDs were usually lower in UCs than in rural areas due to the cold and dry climate. (4) The standard deviations of EVI and WSA (winter) were lower in UCs than in rural areas in most cities in China. Comparatively, nearly all of the findings were less evident in hot and humid Southern China.

This study revealed an interesting characteristic of urban surface, which was helpful for better understanding the urban environment and the relationships between SUHII and climate variability. In present study, urban surface was less sensitive to climate variability than rural in Northern China. However, it does not mean that urbanization is good since it can increase the duration and intensity of heatwaves (and lead to many other environmental issues). In addition, the quantitative impacts of the insensitivity of the urban LST on air temperature, and the relationships between air UHI and climate variability should be comprehensively studied in future.

Acknowledgements

This work was financially supported by National Natural Science Foundation of China (No.41601044), the Special Fund for Basic Scientific Research of Central Colleges, China University of Geosciences, Wuhan (No·CUG150631, CUGL170401), and Opening Foundation of Key Laboratory for National Geograophy State Monitoring (National Administration of Surveying, Mapping and Geoinformation), Key Laboratory of Middle Atmosphere and Global environment Observation (LAGEO) and State Key of Laboratory of Atmospheric Boundary Physics and Atmospheric Chemistry, Institute of Atmospheric Physics, Chinese Academy of Sciences. We would like to thank the China Meteorological Administration (CMA) for providing the meteorological and radiation data.

Appendix A. Supplementary data

Supplementary data to this article can be found online at https://doi.org/10.1016/j.scitotenv.2018.02.087.

References

Akbari, H., Davis, S., Dorsano, S., Huang, J., Winnett, S., 1992. Cooling our Communities a Guidebook on Tree Planting and Light-Colored Surfacing. United States Environmental Protection Agency.

Anniballe, R., Bonafoni, S., Pichierri, M., 2014. Spatial and temporal trends of the surface and air heat island over Milan using MODIS data. Remote Sens. Environ. 150, 163–171.

Brown, P.T., Ming, Y., Li, W., Hill, S.A., 2017. Change in the magnitude and mechanisms of global temperature variability with warming. Nat. Clim. Chang. 7, 743–748.

Cao, C., Lee, X., Liu, S., Schultz, N., Xiao, W., Zhang, M., Zhao, L., 2016. Urban heat islands in China enhanced by haze pollution. Nat. Commun. 7, 12509.

Clinton, N., Gong, P., 2013. MODIS detected surface urban heat islands and sinks: global locations and controls. Remote Sens. Environ. 134, 294–304.

Du, H., Wang, D., Wang, Y., Zhao, X., Qin, F., Jiang, H., Cai, Y., 2016. Influences of land cover types, meteorological conditions, anthropogenic heat and urban area on surface urban heat island in the Yangtze River Delta urban agglomeration. Sci. Total Environ. 571, 461–470.

Founda, D., Pierros, F., Petrakis, M., Zerefos, C., 2015. Interdecadal variations and trends of the urban heat island in Athens (Greece) and its response to heat waves. Atmos. Res. 161-162, 1–13.

Goggins, W.B., Chan, E.Y., Ng, E., Ren, C., Chen, L., 2012. Effect modification of the association between short-term meteorological factors and mortality by urban heat islands in Hong Kong. PLoS One 7, e38551.

Grimm, N.B., Faeth, S.H., Golubiewski, N.E., Redman, C.L., Wu, J., Bai, X., Briggs, J.M., 2008. Global change and the ecology of cities. Science 319, 756–760.

Haashemi, S., Weng, Q., Darvishi, A., Alavipanah, S., 2016. Seasonal variations of the surface urban heat island in a semi-Arid City. Remote Sens. 8, 352.

Han, G., Xu, J., 2013. Land surface phenology and land surface temperature changes along an urban-rural gradient in Yangtze River Delta, china. Environ. Manag. 52, 234–249.

He, T., Liang, S., Wang, D., Wu, H., Yu, Y., Wang, J., 2012. Estimation of surface albedo and directional reflectance from Moderate Resolution Imaging Spectroradiometer (MODIS) observations. Remote Sens. Environ. 119, 286–300.

Hu, L., Monaghan, A., Voogt, J.A., Barlage, M., 2016. A first satellite-based observational assessment of urban thermal anisotropy. Remote Sens. Environ. 181, 111–121.

Huang, J., Yu, H., Dai, A., Wei, Y., Kang, L., 2017a. Drylands face potential threat under 2 °C global warming target. Nat. Clim. Chang. 7, 417–422.

Huang, J., Li, Y., Fu, C., Chen, F., Fu, Q., Dai, A., Shinoda, M., Ma, Z., Guo, W., Li, Z., et al., 2017b. Dryland climate change: recent progress and challenges. Rev. Geophys. 55, 719–778.

Huete, A., Didan, K., Miura, T., Rodriguez, E.P., Gao, X., Ferreira, L.G., 2002. Overview of the radiometric and biophysical performance of the MODIS vegetation indices. Remote Sens. Environ. 83, 195–213.

Imhoff, M.L., Zhang, P., Wolfe, R.E., Bounoua, L., 2010. Remote sensing of the urban heat island effect across biomes in the continental USA. Remote Sens. Environ. 114, 504–513.

IPCC, 2015. Climate Change 2014: Mitigation of Climate Change. Cambridge University Press, UK.

Kolokotroni, M., Ren, X., Davies, M., Mavrogianni, A., 2012. London's urban heat island: impact on current and future energy consumption in office buildings. Energ. Buildings. 47, 302–311.

Kuang, W., Liu, J., Dong, J., Chi, W., Zhang, C., 2016. The rapid and massive urban and industrial land expansions in China between 1990 and 2010: a CLUD-based analysis of their trajectories, patterns, and drivers. Landsc. Urban Plan. 145, 21–33.

Landscheidt, T., 2003. New little ice age instead of global warming? Energ. Environ. 14 (2–3), 327–350.

Li, D., Bou-Zeid, E., 2013. Synergistic interactions between urban heat islands and heat waves: the impact in cities is larger than the sum of its parts*. J. Appl. Meteorol. Climatol. 52, 2051–2064.

Li, D., Sun, T., Liu, M., Yang, L., Wang, L., Gao, Z., 2015. Contrasting responses of urban and rural surface energy budgets to heat waves explain synergies between urban heat islands and heat waves. Environ. Res. Lett. 10, 054009.

Li, D., Sun, T., Liu, M., Wang, L., Gao, Z., 2016. Changes in wind speed under heat waves enhance urban heat islands in the Beijing metropolitan area. J. Appl. Meteorol. Climatol. 55, 2369–2375.

Liang, S., Fang, H., Chen, M., Shuey, C.J., Walthall, C., Daughtry, C., Morisette, J., Schaaf, C., Strahler, A., 2002. Validating MODIS land surface reflectance and albedo products: methods and preliminary results. Remote Sens. Environ. 83, 149–162.

Linares, C., Mirón, I.J., Carmona, R., Sánchez, R., Díaz, J., 2015. Time trend in natural-cause, circulatory-cause and respiratory-cause mortality associated with cold waves in Spain, 1975–2008. Stoch. Env. Res. Risk A. 30, 1565–1574.

Liu, J., Zhang, Z., Xu, X., Kuang, W., Zhou, W., Zhang, S., Li, R., Yan, C., Yu, D., Wu, S., Jiang, N., 2010. Spatial patterns and driving forces of land use change in China during the early 21st century. J. Geogr. Sci. 20, 483–494.

Liu, J., Kuang, W., Zhang, Z., Xu, X., Qin, Y., Ning, J., Zhou, W., Zhang, S., Li, R., Yan, C., Wu, S., Shi, X., Jiang, N., Yu, D., Pan, X., Chi, W., 2014. Spatiotemporal characteristics, patterns, and causes of land-use changes in China since the late 1980s. J. Geogr. Sci. 24, 195–210.

Luo, M., Lau, N.-C., 2017. Heat waves in southern China: synoptic behavior, long-term change, and urbanization effects. J. Clim. 30, 703–720.

Mohan, M., Kandya, A., 2015. Impact of urbanization and land-use/land-cover change on diurnal temperature range: a case study of tropical urban airshed of India using remote sensing data. Sci. Total Environ. 506-507, 453–465.

Nevett, J., 2016. Sun goes blank AGAIN as scientists fear new ICE AGE by 2019. Avalaible at. https://www.dailystar.co.uk/news/latest-news/550344/ice-age-sun-goes-blank-scientists, Accessed date: 13 November 2017.

Peng, S., Piao, S., Ciais, P., Friedlingstein, P., Ottle, C., Breon, F.M., Nan, H., Zhou, L., Myneni, R.B., 2012. Surface urban heat island across 419 global big cities. Environ. Sci. Technol. 46, 696–703.

Piao, S., 2003. Interannual variations of monthly and seasonal normalized difference vegetation index (NDVI) in China from 1982 to 1999. J. Geophys. Res. 108.

Ramamurthy, P., Bou-Zeid, E., 2017. Heatwaves and urban heat islands: a comparative analysis of multiple cities. J. Geophys. Res.-Atmos. 122, 168–178.

Ramamurthy, P., Li, D., Bou-Zeid, E., 2015. High-resolution simulation of heatwave events in New York City. Theor. Appl. Climatol. 128, 89–102.

Santamouris, M., 2015. Analyzing the heat island magnitude and characteristics in one hundred Asian and Australian cities and regions. Sci. Total Environ. 512–513, 582–598.

Schatz, J., Kucharik, C.J., 2015. Urban climate effects on extreme temperatures in Madison, Wisconsin, USA. Environ. Res. Lett. 10, 094024.

Shepherd, S.J., Zharkov, S.I., Zharkova, V.V., 2014. Prediction of solar activity from solar background magnetic field variations in cycles 21–23. Astrophys. J. 795, 46.

Sun, Y., Zhang, X., Ren, G., Zwiers, F.W., Hu, T., 2016. Contribution of urbanization to warming in China. Nat. Clim. Chang. 6, 706–709.

Taheri Shahraiyni, H., Sodoudi, S., El-Zafarany, A., Abou El Seoud, T., Ashraf, H., Krone, K., 2016. A comprehensive statistical study on daytime surface urban heat island during summer in urban areas, case study: Cairo and its new towns. Remote Sens. 8, 643.

United Nations, 2014. World Urbanization Prospects: The 2013 Revision.

Wan, Z., 2008. New refinements and validation of the MODIS land-surface temperature/emissivity products. Remote Sens. Environ. 112, 59–74.

Wan, Z., 2014. New refinements and validation of the collection-6 MODIS land-surface temperature/emissivity product. Remote Sens. Environ. 140, 36–45.

Wang, F., Ge, Q., Wang, S., Li, Q., Jones, P.D., 2015. A new estimation of urbanization's contribution to the warming trend in China. J. Clim. 28, 8923–8938.

Wang, J., Huang, B., Fu, D., Atkinson, P., 2015. Spatiotemporal variation in surface urban heat island intensity and associated determinants across major Chinese cities. Remote Sens. 7, 3670–3689.

Ward, K., Lauf, S., Kleinschmit, B., Endlicher, W., 2016. Heat waves and urban heat islands in Europe: a review of relevant drivers. Sci. Total Environ. 569-570, 527–539.

Weng, Q., 2009. Thermal infrared remote sensing for urban climate and environmental studies: methods, applications, and trends. ISPRS J. Photogramm. Remote Sens. 64, 335–344.

Weng, Q., Fu, P., 2014. Modeling annual parameters of clear-sky land surface temperature variations and evaluating the impact of cloud cover using time series of Landsat TIR data. Remote Sens. Environ. 140, 267–278.

Winguth, A.M.E., Kelp, B., 2013. The urban heat island of the North-Central Texas region and its relation to the 2011 severe Texas drought. J. Appl. Meteorol. Climatol. 52, 2418–2433.

Yao, R., Wang, L., Gui, X., Zheng, Y., Zhang, H., Huang, X., 2017a. Urbanization effects on vegetation and surface urban heat islands in China's Yangtze River basin. Remote Sens. 9, 540.

Yao, R., Wang, L., Huang, X., Guo, X., Niu, Z., Liu, H., 2017b. Investigation of urbanization effects on land surface phenology in Northeast China during 2001–2015. Remote Sens. 9, 66.

Yao, R., Wang, L., Huang, X., Niu, Z., Liu, F., Wang, Q., 2017c. Temporal trends of surface urban heat islands and associated determinants in major Chinese cities. Sci. Total Environ. 609, 742–754.

Zhang, X., Friedl, M.A., Schaaf, C.B., Strahler, A.H., Schneider, A., 2004. The footprint of urban climates on vegetation phenology. Geophys. Res. Lett. 31.

Zhang, P., Imhoff, M.L., Wolfe, R.E., Bounoua, L., 2014. Characterizing urban heat islands of global settlements using MODIS and nighttime lights products. Can. J. Remote. Sens. 36, 185–196.

Zhou, D., Zhao, S., Liu, S., Zhang, L., Zhu, C., 2014. Surface urban heat island in China's 32 major cities: spatial patterns and drivers. Remote Sens. Environ. 152, 51–61.

Zhou, D., Zhao, S., Zhang, L., Sun, G., Liu, Y., 2015. The footprint of urban heat island effect in China. Sci. Rep. 5, 11160.

Zhou, D., Zhang, L., Hao, L., Sun, G., Liu, Y., Zhu, C., 2016a. Spatiotemporal trends of urban heat island effect along the urban development intensity gradient in China. Sci. Total Environ. 544, 617–626.

Zhou, D., Zhang, L., Li, D., Huang, D., Zhu, C., 2016b. Climate–vegetation control on the diurnal and seasonal variations of surface urban heat islands in China. Environ. Res. Lett. 11, 074009.

Zhou, D., Zhao, S., Zhang, L., Liu, S., 2016c. Remotely sensed assessment of urbanization effects on vegetation phenology in China's 32 major cities. Remote Sens. Environ. 176, 272–281.